

Novel Histone Deacetylase Inhibitors: Design, Synthesis, Enzyme Inhibition, and Binding Mode Study of SAHA-Based Non-hydroxamates

Takayoshi Suzuki,^a Yuki Nagano,^a Azusa Matsuura,^a Arihiro Kohara,^b Shin-ichi Ninomiya,^b Kohfuku Kohda^a and Naoki Miyata^{a,*}

^aGraduate School of Pharmaceutical Sciences, Nagoya City University, 3-1 Tanabe-dori, Mizuho-ku, Nagoya, Aichi 467-8603, Japan

^bDaiichi Pure Chemicals Co., Ltd., 2117 Muramatsu, Tokai, Ibaraki 319-1182, Japan

Received 26 August 2003; revised 19 September 2003; accepted 22 September 2003

Abstract—In order to find novel non-hydroxamate histone deacetylase (HDAC) inhibitors, a series of compounds modeled after suberoylanilide hydroxamic acid (SAHA) were designed and synthesized as (i) substrate (acetyl lysine) analogues (compounds 3–7), (ii) analogues bearing various functional groups expected to chelate zinc ion (compounds 8–15), and (iii) analogues bearing nucleophilic functional groups which could bind covalently to HDACs (compounds 16–18). In this series, semicarbazide **8b** and bromoacetamides **18b,c** were found to be potent HDAC inhibitors for non-hydroxamates.

© 2003 Elsevier Ltd. All rights reserved.

Histone deacetylases (HDACs) are known to play an important role in the regulation of gene expression¹ by catalyzing the deacetylation of the acetylated ε-amino groups of specific histone lysine residues.^{2–4} In addition, HDAC inhibitors such as trichostatin A (TSA), suberoylanilide hydroxamic acid (SAHA), and Trapoxin B (TPX B) (Fig. 1) have been reported to inhibit cell growth,^{5–8} induce terminal differentiation in tumor cells,^{5,6} and prevent the formation of tumors in mice.⁹ Therefore, HDACs have emerged as an attractive target for the development of new anticancer drugs. A number of structurally diverse HDAC inhibitors have been reported¹⁰ and most of them belong to hydroxamic acid derivatives, typified by TSA and SAHA, which can interact with zinc in the active site.¹¹ Although hydroxamic acids are frequently employed as zinc-binding groups, they often present metabolic and pharmacokinetic problems such as glucuronidation and sulfation that result in a short in vivo half-life.^{12,13} Many hydroxamates are unstable in vivo, and are prone to hydrolysis giving hydroxylamine which has potential mutagenic properties.¹⁴ Because of such concerns with the

metabolic stability and the toxicity associated with hydroxamic acids, it has become increasingly desirable to find replacement groups that possess strong inhibitory action against HDACs. In addition, in terms of biological research, the discovery of specific irreversible HDAC inhibitors by the replacement of a hydroxamic acid with reactive functional groups will lead to the identification of a new type of biological probe for the isolation and cloning of an HDAC.¹⁵ To date, with the exception of natural macrocyclic products which are not suitable for oral administration, *o*-aminoanilides^{16–18}

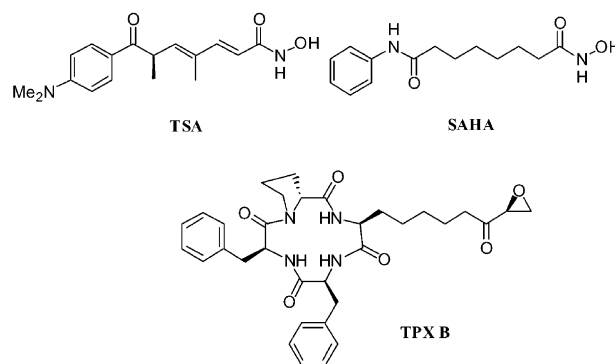


Figure 1. HDAC inhibitors.

*Corresponding author. Tel./fax: +81-52-836-3407; e-mail: miyata-n@phar.nagoya-cu.ac.jp

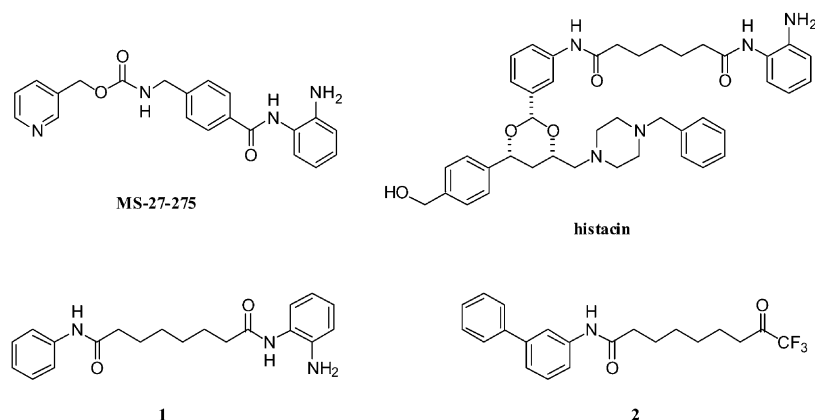


Figure 2. Synthetic non-hydroxamate HDAC inhibitors.

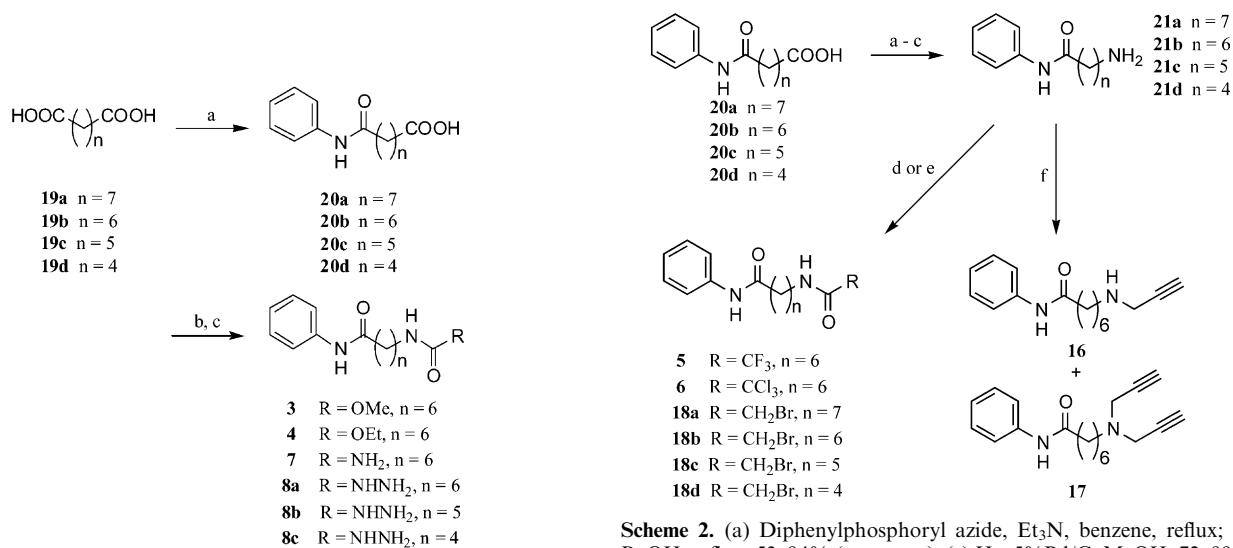
and trifluoromethylketones¹⁹ (Fig. 2) have been reported as non-hydroxamate HDAC inhibitors, and MS-27-275¹⁶ bearing *o*-aminoanilide is currently undergoing evaluation in clinical trials. However, *o*-aminoanilides and trifluoromethylketones have reduced potency as compared to hydroxamate inhibitors, and what is worse, trifluoromethylketones have a metabolic problem in that they are readily reduced to inactive alcohols *in vivo*, even within cells.¹⁹ We therefore initiated a search for replacement groups of hydroxamic acid, other than *o*-aminoanilide and trifluoromethylketone, with the goal of drug discovery as well as finding new tools for biological research. In this letter, we report the design, synthesis, HDAC inhibition, and binding mode analysis of non-hydroxamates based on the structure of SAHA.

A series of compounds modeled after SAHA were synthesized as schematized in Schemes 1–4. Compounds **3**, **4**, **7**, and **8a–c** were synthesized from the corresponding dicarboxylic acids **19b–d** by the route shown in Scheme 1. The condensation of dicarboxylic acids **19a–d** with an

equivalent amount of aniline gave mono-anilides **20a–d**. Curtius rearrangement of carboxylic acids **20b–d** using diphenylphosphoryl azide²⁰ provided the isocyanates, which on treatment with an appropriate alcohol or amine gave carbamates **3**, **4**, urea **7**, and semicabazides **8a–c**.

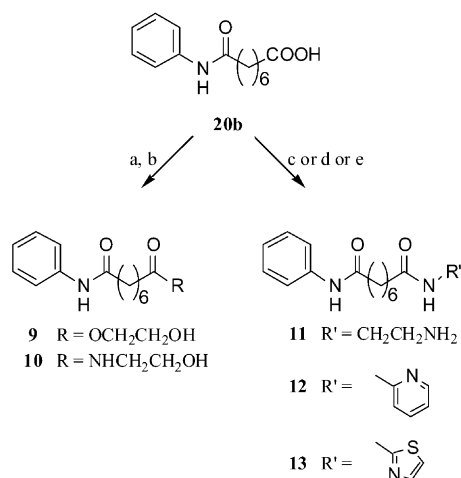
Compounds **5**, **6**, **16**, **17**, and **18a–d** were prepared from carboxylic acids **20a–d** obtained above by the procedure outlined in Scheme 2. Carboxylic acids **20a–d** were converted to amines **21a–d** with a three step sequence: Curtius rearrangement of carboxylic acids **20a–d**, treatment of the resulting isocyanates with benzyl alcohol, and cleavage of the *Z* group by hydrogenation. Coupling between amines **21a–d** and an appropriate acid anhydride or bromoacetyl bromide afforded compounds **5**, **6**, and **18a–d**. The amine **21b** was reacted with propargyl bromide in the presence of K₂CO₃ to give mono- and di-alkylated compounds **16** and **17**.

Compounds **9–12**, and **13** were obtained using standard methodology (Scheme 3). Carboxylic acid **20b** was treated

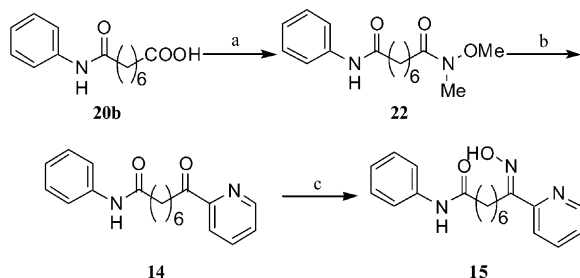


Scheme 1. (a) Aniline, 180 °C, 46–54%; (b) diphenylphosphoryl azide, Et₃N, benzene, reflux; (c) R'OH or R'NH₂, reflux, 24–97% (two steps).

Scheme 2. (a) Diphenylphosphoryl azide, Et₃N, benzene, reflux; (b) BnOH, reflux, 53–94% (two steps); (c) H₂, 5%Pd/C, MeOH, 72–99%; (d) TFAA or (CCl₃CO)₂O, Et₃N, CHCl₃, 80% for **5**, 38% for **6**; (e) bromoacetyl bromide, Et₃N, THF, 22–41%; (f) propargyl bromide, K₂CO₃, MeOH, 58% (**16**), 17% (**17**).



Scheme 3. (a) ClCOOMe, Et₃N, THF; (b) ethyleneglycol or aminoethanol, CH₂SO₄, 84% for **9**, 48% for **10** (two steps); (c) ethylenediamine, EDCI, NHS, CHCl₃, 49%; (d) 2-aminopyridine, 1*H*-benzotriazol-1-yloxytripyrrolidinophosphonium hexafluorophosphate (PyBOP[®]), DMF, 85%; (e) 2-aminothiazole, EDCI, HOBT, DMF, 95%.



Scheme 4. (a) *N,O*-Dimethylhydroxylamine hydrochloride, Et₃N, EDCI, HOBT, DMF, 85%; (b) 2-bromopyridine, *n*-BuLi, THF, −78 °C, 88%; (c) hydroxylamine hydrochloride, pyridine, EtOH, 90%.

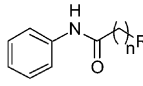
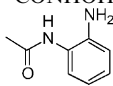
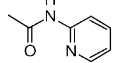
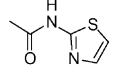
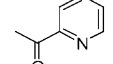
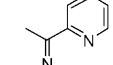
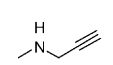
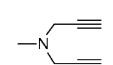
with methyl chloroformate followed by ethyleneglycol or aminoethanol to yield ester **9** and amide **10**. Amides **11**, **12**, and **13** were obtained by the condensation of carboxylic acid **20b** with an appropriate amine in the presence of condensing reagents such as EDCI and HOBT.

Synthesis of ketone **14** was accomplished via Weinreb amide²¹ **22** as shown in **Scheme 4**. Carboxylic acid **20b** was converted to Weinreb amide **22** using the procedure employed in the preparation of **13**. Compound **22** was allowed to react with 2-pyridinyl lithium at −78 °C to give ketone **14** and subsequent oxime formation afforded compound **15**. The stereochemistry of oxime **15** was determined to be *E* by following the Beckmann rearrangement method.^{22,23} More specifically, treatment of **15** with PCl₅ in dichloromethane at room temperature yielded amide **12**.

The compounds synthesized in this study were tested with an in vitro assay using a HeLa nuclear extract, rich in HDAC activity.²⁴ The results are summarized in **Table 1**.

The IC₅₀ values of SAHA and *o*-aminoanilide **1** were 0.28 and 120 μM, respectively (entries 1 and 2). Newly

Table 1. HDAC inhibition data for SAHA and SAHA-based non-hydroxamates^a

Entry	Comp	R	<i>n</i>	<div>  </div>	
				% Inhib at 100 μM	IC ₅₀ (μM)
1	SAHA ^b	−CONHOH	6	100	0.28
2	1		6	48	120
3	3	−NHCOOMe	6	12	> 100
4	4	−NHCOOEt	6	19	> 100
5	5	−NHCOCF ₃	6	3	> 100
6	6	−NHCOCCl ₃	6	4	> 100
7	7	−NHCONH ₂	6	7	> 100
8	8a	−NHCONHNH ₂	6	18	650
9	8b	−NHCONHNH ₂	5	35	150
10	8c	−NHCONHNH ₂	4	12	> 1000
11	9	−COOCH ₂ CH ₂ OH	6	5	> 100
12	10	−CONHCH ₂ CH ₂ OH	6	4	> 100
13	11	−CONHCH ₂ CH ₂ NH ₂	6	3	> 100
14	12		6	8	> 100
15	13		6	9	> 100
16	14		6	15	> 100
17	15		6	0	> 100
18	16		6	16	> 100
19	17		6	8	> 100
20	18a	−NHCOCH ₂ Br	7	40	300
21	18b	−NHCOCH ₂ Br	6	79	14
22	18c	−NHCOCH ₂ Br	5	78	17
23	18d	−NHCOCH ₂ Br	4	47	121

^aValues are means of at least three experiments.

^bPrepared as described in *ref 31*.

synthesized acetyl lysine-like derivatives **3–7** expected to inhibit HDACs competitively were found to be totally inactive or only weakly potent against HDACs (entries 3–7).

The crystal structure of an archaeobacterial HDAC homologue (HDAC-like protein, HDLP)/SAHA complex made it clear that the hydroxamic acid group coordinates the zinc ion through its CO and OH groups and also forms three hydrogen bonds between its CO, NH, OH groups and Tyr 297, His 132, His 131, respectively.¹¹ From these data, semicarbazide **8b** was synthesized and tested as an HDAC inhibitor because it is possible for semicarbazide to chelate metal ions and form hydrogen bonds with Tyr and His. As was expected, **8b** showed anti-HDAC activity and the IC₅₀ value was comparable to that of *o*-aminoanilide **1** (entry 9).

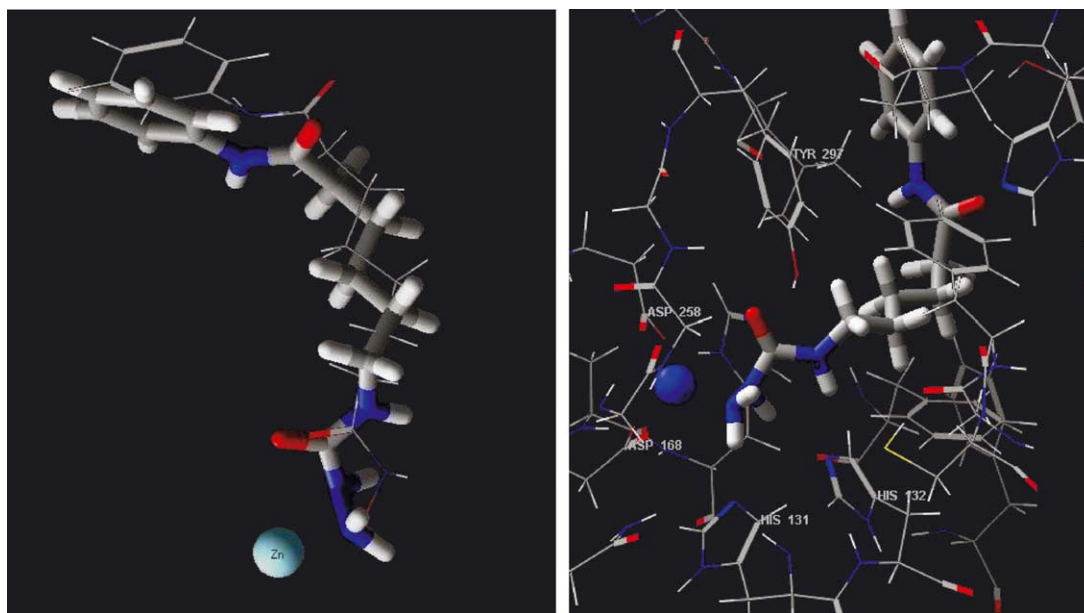


Figure 3. Superposition of the low energy conformations of **8b** (tube) and SAHA (wire) (left). The HDLP pocket is not shown for the sake of clarity. View of the conformation of **8b** (tube) docked into the HDLP catalytic core (right). Residues 5 Å from the ligand are displayed in the wire graphic.

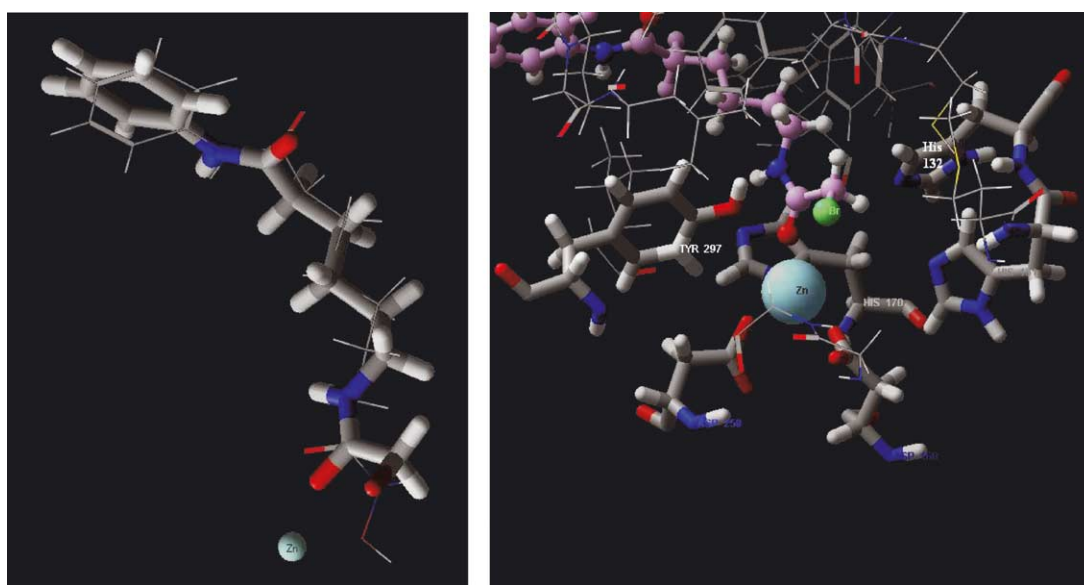


Figure 4. Superposition of the low energy conformations of **18c** (tube) and SAHA (wire) (left). The HDLP pocket is not shown for the sake of clarity. View of the conformation of **18c** (ball and stick) docked into the HDLP catalytic core (right). Residues within 5 Å of the zinc ion are displayed in the tube graphic.

The potency of semicarbazides **8a–c** was directly related to chain length, and the most potent compound was **8b**, where $n=5$ (entries 8–10). To find more potent zinc-binding groups, we examined the simplified analogues (**9–11**) of *o*-aminoanilide **1** in which the benzene ring is replaced by an ethylene chain, but these compounds had lost HDAC inhibitory activities (entries 11–13). These results suggest that the benzene ring of **1** is required to fix the position of its amino group or to interact with amino acid residues of the enzyme. Since the effect of the benzene ring of **1** proved to be influential, we introduced heteroaryl rings as zinc-binding groups (**12–15**). Although arylamide, the 2-acylated heteroaryl ring, and the oxime have been reported to coordinate zinc ion in a

bidentate fashion through the hetero atom of the heteroaryl ring and the carbonyl/oxime group,^{14,25,26} all heteroaryl compounds proved to be less effective than *o*-aminoanilide **1** in inhibiting the enzyme at 100 μM (entries 14–17).

We turned our attention to irreversible HDAC inhibitors. TPX B is an irreversible HDAC inhibitor,⁸ but finding more specific and simpler irreversible HDAC inhibitors is useful for the isolation and cloning of an HDAC.¹⁵ As described above, the crystal structure of HDLP/SAHA complex revealed that the hydroxamic acid group forms three hydrogen bonds with Tyr 297, His 132, and His 131, and furthermore, zinc ion is

coordinated by His 170, Asp 168, and Asp 258. Since the phenol group of Tyr, the imidazole group of His, and the carboxyl group of Asp are able to react with electrophiles, we prepared analogues bearing propargyl amino (**16**, **17**) and bromoacetamide (**18b**) which could bind covalently to Tyr, His, and Asp of the enzyme, and evaluated their anti-HDAC activities. While propargyl amino compounds **16** and **17** did not possess HDAC inhibitory activities, potent inhibition was observed with bromoacetamide **18b** (entries 18, 19, and 21). Bromoacetamide **18b** exhibited an IC_{50} of 14 μ M and its activity largely surpassed that of *o*-aminoanilide **1**. HDAC inhibition was distinctly dependent on chain length within the bromoacetamide series, with $n=7$ (**18a**) and $n=4$ (**18d**) resulting in less potent inhibitors. However, **18c**, in which $n=5$, proved to be at least equally effective to **18b**, in which $n=6$ (entries 20–23).

To study the binding mode of compounds **8b** and **18c** in the active site, we calculated the low energy conformations of **8b** and **18c** when they are docked into the model based on the crystal structure of HDLP (PDB code 1C3R) using the software packages Macromodel 8.0,²⁷ and compared the results with those obtained with SAHA. First, the binding mode of **8b** was investigated. The anilide group and alkyl chain of **8b** and SAHA are essentially superimposed in the binding pocket (Fig. 3, left), and the binding mode of **8b** is similar to that of SAHA (Fig. 3, right). An inspection of the HDLP/**8b** complex shows that the semicarbazide moiety of **8b** was slightly removed from the zinc ion (CO–Zn, 3.1 Å; NH₂–Zn, 2.1 Å), whereas the hydroxamic acid group of SAHA was positioned at the optimal bond distance (CO–Zn, 2.7 Å; OH–Zn, 1.8 Å). Next, we investigated the binding mode of **18c**. As is the case with **8b**, the anilide group and alkyl chain of **18c** and SAHA are superimposed in the binding pocket (Fig. 4, left). In the case of **18c**, only the carbonyl group of bromoacetamide chelates zinc ion as shown in Figure 4, right. Because **18c** is thought to be an irreversible inhibitor, **18c** may inhibit HDACs by forming a covalent bond with His 132 lying next to the reactive site of the bromoacetamide.

In summary, in order to find novel non-hydroxamate HDAC inhibitors, we designed and prepared SAHA-based compounds as (i) substrate (acetyl lysine) analogues (compounds **3–7**), (ii) analogues bearing various functional groups expected to chelate zinc ion (compounds **8–15**), and (iii) analogues bearing nucleophilic functional groups which could bind covalently to HDACs (compounds **16–18**). In zinc coordination-oriented series, semicarbazide **8b** was found to be as potent as *o*-aminoanilide **1**, and we have shown that the potency is related to chain length, with $n=5$ optimal. Molecular modeling suggests that the binding mode of **8b** is similar to that of SAHA. As far as we could determine, this is the first report of semicarbazide as a zinc-dependent enzyme inhibitor. The semicarbazide group may be useful as a source of other zinc-dependent enzyme inhibitors such as matrix metalloproteinase inhibitors,^{14,28} tumor necrosis factor- α converting enzyme inhibitors,²⁹ and aggrecanase inhibitors.³⁰ In the irreversible inhibition-oriented series, bromoacet-

amides **18b** and **18c** proved to be the strongest HDAC inhibitors of all non-hydroxamate inhibitors prepared for this study. HDAC inhibition was also distinctly dependent on chain length within the bromoacetamide series, with $n=5$ and 6 optimal. The binding mode analysis of **18c** suggests that **18c** may inhibit HDACs by forming a covalent bond with His 132. More specific irreversible HDAC inhibitors can be used for the isolation and cloning of an HDAC.¹⁵ Further investigation and a detailed inhibitory mechanism analysis pertaining to **8b** and **18b,c** are under way.

Acknowledgements

This work was supported in part by a grant from the Health Sciences Foundation from the Ministry of Health, Labor and Welfare of Japan.

References and Notes

1. Davie, J. R.; Chadee, D. N. *J. Cell. Biochem.* **1998**, 30–31 (Suppl), 203.
2. Grunstein, M. *Nature* **1997**, 389, 349.
3. Ng, H. H.; Bird, A. *Trends Biochem. Sci.* **2000**, 25, 121.
4. Cheung, W. L.; Briggs, S. D.; Allis, C. D. *Curr. Opin. Cell. Biol.* **2000**, 12, 326.
5. Yoshida, M.; Horinouchi, S.; Beppu, T. *BioEssays* **1995**, 17, 423.
6. Richon, V. M.; Webb, Y.; Merger, R.; Sheppard, T.; Jursic, B.; Ngo, L.; Civoli, F.; Breslow, R.; Rifkind, R. A.; Marks, P. A. *Proc. Natl. Acad. Sci. U.S.A.* **1996**, 93, 5705.
7. Richon, V. M.; Emiliani, S.; Verdin, E.; Webb, Y.; Breslow, R.; Rifkind, R. A.; Marks, P. A. *Proc. Natl. Acad. Sci. U.S.A.* **1998**, 95, 3003.
8. Kijima, M.; Yoshida, M.; Sugita, K.; Horinouchi, S.; Beppu, T. *J. Biol. Chem.* **1993**, 268, 22429.
9. Cohen, L. A.; Amin, S.; Marks, P. A.; Rifkind, R. A.; Desai, D.; Richon, V. M. *Anticancer Res.* **1999**, 19, 4999.
10. Jung, M. *Curr. Med. Chem.* **2001**, 8, 1505.
11. Finnin, M. S.; Donigian, J. R.; Cohen, A.; Richon, V. M.; Rifkind, R. A.; Marks, P. A.; Breslow, R.; Pavletich, N. P. *Nature* **1999**, 401, 188.
12. Mulder, G. J.; Meerman, J. H. *Environ. Health Perspect.* **1983**, 49, 27.
13. Vassiliou, S.; Mucha, A.; Cuniasse, P.; Georgiadis, D.; Lucet-Levannier, K.; Beau, F.; Kannan, R.; Murphy, G.; Knaeuper, V.; Rio, M. C.; Basset, P.; Yiotakis, A.; Dive, V. J. *Med. Chem.* **1999**, 42, 2610.
14. Whittaker, M.; Floyd, C. D.; Brown, P.; Gearing, A. J. *Chem. Rev.* **1999**, 99, 2735.
15. Taunton, J.; Hassig, C. A.; Schreiber, S. L. *Science* **1996**, 272, 408.
16. Saito, A.; Yamashita, T.; Mariko, Y.; Nosaka, Y.; Tsuchiya, K.; Ando, T.; Suzuki, T.; Tsuruno, T.; Nakanishi, O. *Proc. Natl. Acad. Sci. U.S.A.* **1999**, 96, 4592.
17. Wong, J. C.; Hong, R.; Schreiber, S. L. *J. Am. Chem. Soc.* **2003**, 125, 5586.
18. Haggarty, S. J.; Koeller, K. M.; Wong, J. C.; Butcher, R. A.; Schreiber, S. L. *Chem. Biol.* **2003**, 10, 383.
19. Frey, R. R.; Wada, C. K.; Garland, R. B.; Curtin, M. L.; Michaelides, M. R.; Li, J.; Pease, L. J.; Glaser, K. B.; Marcotte, P. A.; Bouska, J. J.; Murphy, S. S.; Davidsen, S. K. *Bioorg. Med. Chem. Lett.* **2002**, 12, 3443.

20. Shioiri, T.; Ninomiya, K.; Yamada, S. *J. Am. Chem. Soc.* **1972**, *94*, 6203.
21. Nahm, S.; Weinreb, S. M. *Tetrahedron Lett.* **1981**, *22*, 3815.
22. Huntress, E. H.; Walter, H. C. *J. Am. Chem. Soc.* **1948**, *70*, 3702.
23. Negi, S.; Matsukura, M.; Mizuno, M.; Miyake, K.; Minami, N. *Synthesis* **1996**, 991.
24. HDAC activity assay was performed using the HDAC fluorescent activity assay/drug discovery kit (AK-500, BIO-MOL Research Laboratories): HeLa Nuclear Extract (0.5 μ L/well) were incubated (37°C) with 25 μ M of Fluor de LysTM substrate and various concentrations of samples. Reactions were stopped after 30 min. with Fluor de LysTM Developer and fluorescence was measured on a fluorometric reader with excitation set at 360 nm and emission detection set at 460 nm.
25. Augé, F.; Hornebeck, W.; Decarme, M.; Laronze, J.-Y. *Bioorg. Med. Chem. Lett.* **2003**, *13*, 1783.
26. Cooperman, B. S.; Lloyd, G. J. *J. Am. Chem. Soc.* **1971**, *93*, 4883.
27. Mohamadi, F.; Richards, N. G. J.; Guida, W. C.; Liskamp, R.; Lipton, M.; Caufield, C.; Chang, G.; Hendrickson, T.; Still, W. C. *J. Comput. Chem.* **1990**, *11*, 440.
28. Skiles, J. W.; Gonnella, N. C.; Jeng, A. Y. *Curr. Med. Chem.* **2001**, *8*, 425.
29. Chen, J. M.; Jin, G.; Sung, A.; Levin, J. I. *Bioorg. Med. Chem. Lett.* **2002**, *12*, 1195.
30. Yao, W.; Chao, M.; Wasserman, Z. R.; Liu, R.-Q.; Covington, M. B.; Newton, R.; Christ, D.; Wexler, R. R.; Decicco, C. P. *Bioorg. Med. Chem. Lett.* **2002**, *12*, 101.
31. Mai, A.; Esposito, M.; Sbardella, G.; Massa, S. *Org. Prep. Proced. Int.* **2001**, *33*, 391.